Improved Admittance Matrix Estimation on Power Networks Based on Hybrid Measurements

Yixiong Jia[1], *Student Member, IEEE*, Yu Liu[1,*], *Member, IEEE*, Dayou Lu[1], *Student Member, IEEE*, and Zhibo Cao[1], *Student Member, IEEE*
1. School of Information Science and Technology, ShanghaiTech University, Shanghai, China
*corresponding author: liuyu.shanghaitech@gmail.com

***Abstract*: This paper proposes an improved admittance matrix estimation method on power networks based on hybrid measurements. The method only requires voltage magnitude measurements for the most buses, and PMU measurements are only placed on very limited number of buses. The proposed approach first improves the existing admittance matrix estimation method via establishing a new model of the power networks under estimation, with system voltage phasors and the admittance matrix as the unknown states. Afterwards, the model is solved through the Newton's method to obtain the admittance matrix. Numerical experiments validates that accurate and reliable estimation of the admittance matrix can be achieved using the proposed method. The method also demonstrates robustness towards measurement errors.**
Index Terms*: *admittance matrix estimation, hybrid measurements, PMU measurements, voltage magnitude measurements

I. Introduction

Parameters of power system networks (for example series resistance, series reactance and shunt admittance) are usually provided by the utilities. Nevertheless, in practice these parameters may not be quite accurate in the utility database. Furthermore, the values of parameters could be easily affected by environmental factors like temperature or weather, human activities and usage time [1-2]. Therefore, line parameters in the power networks always vary from the nominal values: there could be even 25%-30% differences between the actual values and the nominal values [3]. This leads to problematic results for many applications such as power flow calculation, transmission line protection, fault location etc., since these applications in the power networks require accurate line parameters. As a result, an accurate and reliable line parameters estimation method of the power networks is of great importance. To solve this problem, researchers proposed a series of methods for parameter estimation, and can be mainly classified into classical estimation schemes and network estimation schemes.

Classical estimation methods follow the idea of the conventional two-terminal line parameters estimation in a power network. The concept is to consider any two adjacent buses as a two-terminal system. By using line parameters estimation techniques in a two-terminal system, the branch parameters corresponding to the two-terminal line can be fully estimated. Traveling wave parameter estimation [4] utilizes information of voltage and current waveforms captured by the digital relays to estimate the line parameters. It uses the wave propagation speed equation to make the estimation results more accurate. In [5], the long line parameters are estimated through long line π equivalent circuit; the literature also uses both PMU and SCADA data to make the estimation results more accurate. Literature [6] proposes a time-domain method for estimation of three phase untransposed line parameters by using Kalman filter. Literature [7] estimates line parameters of three phase synchronous system in phasor domain by using ordinary least-squares; it can be applied for both fully transposed and untransposed transmission lines. Note that references [4-7] need to install the PMU at both ends of the line, meaning that we need to install the PMU at the two buses of the line terminals, in order to estimate the line parameters. Nevertheless, the cost could be quite high for large systems. To overcome this shortcoming, literature [8] installs at least one PMU for each line to make the system observable and the measurement of the other end is obtained by the hybrid state estimator. Literature [9] improves the method of [8] and add suspicious lines. However, classical estimation methods do not fully consider the entire topology of the system, leading to compromised parameter estimation accuracy.

Network estimation methods estimate the line parameters with consideration of topology information of the network. For the widely adopted radial power network in China, literature [10] gives a full derivation of the measurement model which considers the information of network topology and measurement constraints. Literature [11] suggests that the branch parameters estimation should be applied to suspicious lines rather than all the systems. However, the suspicious lines cannot be determined in reality. Besides, researchers also proposed methods based on estimating the admittance matrix. The concept is that the voltage vector and current injection vector can be related through admittance matrix, and the admittance matrix can be fully estimated by measuring the voltage and current injection of each bus. Since the bus current injection is equal to zero when the bus is not connected to power sources, these methods do not need to measure the current on most buses compared with classical estimation methods. Paper [12] estimates the admittance matrix from the optimization view by using snapshots. Paper [13] estimates the admittance matrix from the statistic distribution view by using snapshots. Even though network estimation methods fully exploit the topology information of a power network and they can avoid measuring currents on most buses in the system, present methods still require installations of PMUs at all the buses to ensure synchronization, which may still increase costs for a practical power networks.

This paper proposes an improved admittance matrix estimation method on power networks based on hybrid measurements: combinations of PMU measurements and voltage magnitude measurements. Accurate and reliable admittance matrix estimation can be obtained through installing PMUs at a few key buses and measuring the magnitude of the voltage at the rest of the buses. Through this way, the number of PMU can much be reduced and phase angle measurements can be avoided for the most buses, and therefore the proposed method is compatible with the practical power networks. In particular, the proposed method establishes a new model of the power network under estimation, with system voltage phasors and admittance matrix as the unknown states to be estimated. Numerical experiments prove that the proposed method can accurately estimate the admittance matrix on power networks using hybrid measurements.

The remainder of the paper is arranged as follows. Section II gives the fundamental model of the power networks and derives the proposed approach. Section III provides numerical experiments where the performances of the proposed method are examined. Section IV concludes a conclusion.

This work is sponsored by National Nature Science Foundation of China (No. 51807119). The support is greatly appreciated,

II. Proposed Bus Admittance Matrix Estimation Method Based on Hybrid Measurements

In this session, we will first review the fundamental model of the power networks. After that, the proposed bus admittance matrix estimation method based on hybrid measurements will be presented in detail. In fact, the value of admittance matrices may vary due to change of ground resistivity, temperature, weather, etc. Here the admittance matrix to be estimated is assumed as a constant matrix within a short period of time.

A. *Fundamental model of power networks*

For a power network system with *n* buses, the voltage phasors and current injection phasors can be related through an admittance matrix $\boldsymbol{Y}_{bus}$ as show in (1).

$$\boldsymbol{Y}_{bus} \cdot \tilde{\boldsymbol{V}}_{bus} = \tilde{\boldsymbol{I}}_{bus} \tag{1}$$

where $\boldsymbol{Y}_{bus} \in \mathbb{C}^{n \times n}$ is an admittance matrix of the *n* bus system, $\tilde{\boldsymbol{V}}_{bus} \in \mathbb{C}^{n \times 1}$ is a vector containing the voltage phasors at all bus in the *n* bus system, $\tilde{\boldsymbol{I}}_{bus} \in \mathbb{C}^{n \times 1}$ is a vector containing the current injection phasors at all bus in the *n* bus system. Note that if the i^{th} bus is connected to a power source, the i^{th} entry of $\tilde{\boldsymbol{I}}_{bus}$ is non-zero (otherwise the entry of $\tilde{\boldsymbol{I}}_{bus}$ is zero). Therefore, we can classify the buses by the type of measurements, as shown in Table 1. Note that here equation (1) requires phase angle information for voltages and currents; therefore, traditional methods usually utilize PMU measurements. It is also notable that there are two kinds of buses in the system: one kind is the key buses that are connected to the power sources, while the other kind is the normal buses that are not connected to power sources.

Table 1. Bus types of the power networks

Bus type	Measurement
1 (connected to sources)	Voltage and current, PMU measurements
2 (others)	Voltage, PMU measurements

B. *Modeling for Estimation of Bus Admittance Matrix Based on Hybrid Measurements*

From (1) and the Table 1, one can observe that the fundamental model utilizes the voltage PMU measurements at all the buses and the current PMU measurements at the buses that are connected to power sources. It is worth noting that in order to measure the phasor angle of the voltages, we still need to install PMUs even for type 2 buses. However, it is unlikely to place PMUs at all the bus for practical power networks. In order to reduce the number of PMUs installed inside the power networks and avoid measuring voltage phase angles of the type 2 buses, we provide new definitions of bus types as shown in Table 2. For the buses without connection to the sources, we only have voltage magnitude measurements. It is more practical to place the devices that only measure the voltage magnitude in the system for type 2 buses.

Table 2. New definition of bus types

Bus type	Measurement
1 (connected to sources)	Voltage and current, PMU measurements
2 (others)	Magnitude of voltage

Here the PMU measurements are installed on generator buses (type 1 buses) and the voltage magnitude measurements are installed on the other buses (type 2 buses). Note that for the proposed modeling, the minimum number of PMUs is equal to the number of sources (the problem will have more redundancy if PMU measurements are also available on some type 2 buses).

For the following analysis, the measurement installation in Table 2 is taken as examples to ensure the minimum number of PMUs. Note that the real and imaginary parts of the voltage phasors of the type 2 buses are unknown; we only know the voltage magnitude information. In this section, the formulation of the new model and the reason of how it works will be given as follows,

Separate the real and imaginary part of (1), we could get an equivalent formulation (2),

$$\boldsymbol{Y} \cdot \boldsymbol{V} = \boldsymbol{I} \tag{2}$$

where

$$\boldsymbol{Y} = \begin{bmatrix} real(\boldsymbol{Y}_{bus}) & -imag(\boldsymbol{Y}_{bus}) \\ imag(\boldsymbol{Y}_{bus}) & real(\boldsymbol{Y}_{bus}) \end{bmatrix} \in \mathbb{R}^{2\boldsymbol{n} \times 2\boldsymbol{n}},$$

$$\boldsymbol{V} = \begin{bmatrix} real(\tilde{\boldsymbol{V}}_{bus}) \\ imag(\tilde{\boldsymbol{V}}_{bus}) \end{bmatrix} \in \mathbb{R}^{2\boldsymbol{n} \times 1}, \ \boldsymbol{I} = \begin{bmatrix} real(\tilde{\boldsymbol{I}}_{bus}) \\ imag(\tilde{\boldsymbol{I}}_{bus}) \end{bmatrix} \in \mathbb{R}^{2\boldsymbol{n} \times 1},$$

where $real(\bullet)$ denotes the real part of the matrix $(\bullet)$, and $imag(\bullet)$ denotes the imaginary part of the matrix $(\bullet)$.

Next, the proposed method will add extra rows to the admittance matrix as well as the measurement current injection vector. Define the extra rows added into the admittance matrix as 'Phasor Information Matrix': $\boldsymbol{PIM} \in \mathbb{R}^{p \times 2n}$; define the extra rows added into the measurement current injection vector as 'Magnitude Information Matrix': $\boldsymbol{MIM} \in \mathbb{R}^{p \times 1}$. *p* is the number of type 2 buses in the power network (i.e. $p = 6$ in the 9-bus system show in Figure 3 in section III).

The details of ***PIM*** and ***MIM*** are dependent on the indexing of the type 2 buses. For example, the indexing we designed for the 9-bus system in Figure 3 is shown as Table 3.

Table 3. Type 2 bus indexing for the 9-bus system

Type 2 bus number	4	5	6	7	8	9
Row index for the ***PIM*** , ***MIM***	1	2	3	4	5	6

From the Table 3, we will construct ***PIM*** and ***MIM*** step by step as follows. Separate ***PIM*** as $\boldsymbol{PIM} = \begin{bmatrix} \boldsymbol{PIM}_{real} & \boldsymbol{PIM}_{imag} \end{bmatrix}$, where $\boldsymbol{PIM}_{real} \in \mathbb{R}^{p \times n}$ and $\boldsymbol{PIM}_{imag} \in \mathbb{R}^{p \times n}$ containing the real and imaginary part of the voltage phasors of the type 2 buses respectively. With the bus number *g* and the row index for the ***PIM*** and ***MIM*** (the index is represented as variable *k*), ***PIM*** and ***MIM*** can be constructed as,

$$\begin{aligned} &\left[\boldsymbol{PIM}_{real}\right]_{k,g} = real((\tilde{\boldsymbol{V}}_{bus})_{g,1}) \\ &\left[\boldsymbol{PIM}_{imag}\right]_{k,g} = imag((\tilde{\boldsymbol{V}}_{bus})_{g,1}) \\ &\boldsymbol{PIM} = \begin{bmatrix} \boldsymbol{PIM}_{real} & \boldsymbol{PIM}_{imag} \end{bmatrix} \\ &\left[\boldsymbol{MIM}\right]_{k,1} = (real((\tilde{\boldsymbol{V}}_{bus})_{g,1}))^2 + (imag((\tilde{\boldsymbol{V}}_{bus})_{g,1}))^2 \end{aligned} \tag{3}$$

where $\left[\bullet\right]_{j,k}$ represents the value of $\left[\bullet\right]$ at row j, column k.

In order to better understand the relationship between the ***PIM*** and $\boldsymbol{V}$, we just take the 9-bus system as an example. The relationship is shown in Figure 1. From Figure 1, we can see that ***PIM*** contains the real and imaginary part of the type 2 bus voltage phasor. Similarly, to better understand the relationship between the ***MIM*** and $\boldsymbol{V}$, the 9-bus system is also taken as an example. The relationship is shown in Figure 2. From Figure 2, we can see that ***MIM*** contains the squared magnitude of the type 2 bus voltage phasor.

After constructing ***PIM*** and ***MIM***, the final formulation of our proposed method can be derived. Define the augmented matrices $\boldsymbol{Y}_{PIM}$ and $\boldsymbol{I}_{MIM}$ as,

$$\boldsymbol{Y}_{PIM} = \begin{bmatrix} \boldsymbol{Y} \\ \boldsymbol{PIM} \end{bmatrix}, \boldsymbol{I}_{MIM} = \begin{bmatrix} \boldsymbol{I} \\ \boldsymbol{MIM} \end{bmatrix} \tag{4}$$

where $\boldsymbol{Y}_{PIM} \in \mathbb{R}^{(2n+p)\times 2n}$ and $\boldsymbol{I}_{MIM} \in \mathbb{R}^{(2n+p)\times 1}$.

Therefore, equation (2) can be rewritten with the augmented matrices as defined in (5),

$$\boldsymbol{Y}_{PIM} \cdot \boldsymbol{V} = \boldsymbol{I}_{MIM} \tag{5}$$

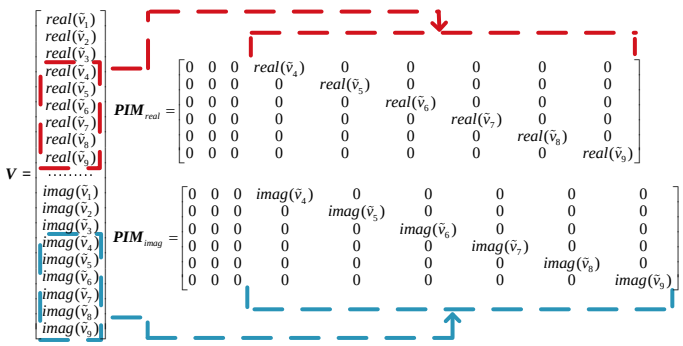

Figure 1. Relationship between $\boldsymbol{V}$ and $\boldsymbol{PIM}$

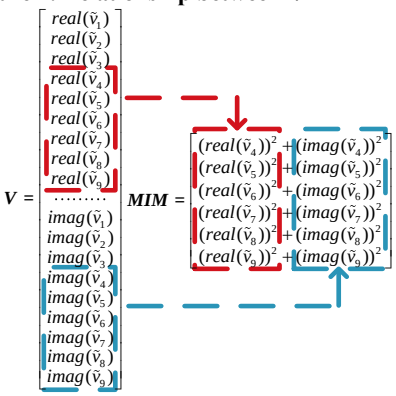

Figure 2. Relationship between $\boldsymbol{V}$ and $\boldsymbol{MIM}$

Assume that the parameters to be estimated are constants within a short period of time. In order to increase redundancy of the parameter estimation problem, the idea of snapshots is applied [10], where each snapshot corresponds to one group of voltage/current measurements. With serval snapshots within a short period of time, we have,

$$\begin{bmatrix} \boldsymbol{Y}_{PIM}^{(1)} & & & \\ & \boldsymbol{Y}_{PIM}^{(2)} & & \\ & & \ddots & \\ & & & \boldsymbol{Y}_{PIM}^{(m)} \end{bmatrix} \cdot \begin{bmatrix} \boldsymbol{V}^{(1)} \\ \boldsymbol{V}^{(2)} \\ \vdots \\ \boldsymbol{V}^{(m)} \end{bmatrix} = \begin{bmatrix} \boldsymbol{I}_{MIM}^{(1)} \\ \boldsymbol{I}_{MIM}^{(2)} \\ \vdots \\ \boldsymbol{I}_{MIM}^{(m)} \end{bmatrix} \tag{6}$$

where m is the number of snapshots, $\boldsymbol{Y}_{PIM}^{(h)} = \begin{bmatrix} \boldsymbol{Y} \\ \boldsymbol{PIM}^{(h)} \end{bmatrix}$, $\boldsymbol{I}_{MIM}^{(h)} = \begin{bmatrix} \boldsymbol{I}^{(h)} \\ \boldsymbol{MIM}^{(h)} \end{bmatrix}$, $\boldsymbol{V}^{(h)} = \begin{bmatrix} real(\tilde{\boldsymbol{V}}_{bus}^{(h)}) \\ imag(\tilde{\boldsymbol{V}}_{bus}^{(h)}) \end{bmatrix}$, and $(\bullet)^{(h)}$ represent the h^{th} snapshots of the matrix or the vector.

In order to simplify the notation, rewrite equation (6) as,

$$\boldsymbol{Y}_{snap} \cdot \boldsymbol{V}_{snap} = \boldsymbol{I}_{snap} \tag{7}$$

where $\boldsymbol{Y}_{snap} = \begin{bmatrix} \boldsymbol{Y}_{PIM}^{(1)} & & & \\ & \boldsymbol{Y}_{PIM}^{(2)} & & \\ & & \ddots & \\ & & & \boldsymbol{Y}_{PIM}^{(m)} \end{bmatrix} \in \mathbb{R}^{(2mn+mp)\times 2mn}$ is a block diagonal matrix whose entries are from $\boldsymbol{Y}_{PIM}^{(1)}$ to $\boldsymbol{Y}_{PIM}^{(m)}$, $\boldsymbol{V}_{snap} \in \mathbb{R}^{2mn\times 1} = [\boldsymbol{V}^{(1)}, \boldsymbol{V}^{(2)}, \cdots, \boldsymbol{V}^{(m)}]^T$, $\boldsymbol{I}_{snap} \in \mathbb{R}^{2nm\times 1} = [\boldsymbol{I}_{MIM}^{(1)}, \boldsymbol{I}_{MIM}^{(2)}, \cdots, \boldsymbol{I}_{MIM}^{(m)}]^T$, the definitions of $\boldsymbol{Y}_{PIM}^{(j)}$, $\boldsymbol{V}^{(j)}$ and $\boldsymbol{I}_{MIM}^{(j)}$ are shown as above, and $j \in [1, m]$.

C. *Parameters Estimation via the Newton's Method*

Next, the way to estimate the admittance matrix $\boldsymbol{Y}_{bus}$ is presented. Rewrite (7) as follows,

$$\boldsymbol{y} = G(\boldsymbol{x}) \tag{8}$$

where $\boldsymbol{y} = \boldsymbol{I}_{snap}$ is the measurement vector (including voltage phasor/current injection phasor measurements of type 1 bus, and squared voltage magnitude measurements of type 2 bus), x is the state vector to be solved. Here the state vector x contains parameters within the matrix $\boldsymbol{Y}_{bus}$ and also the real/imaginary parts of the type 2 bus voltage phasors. For the example 9-bus test system in Figure 3, there are 18 non-zero complex entries in $\boldsymbol{Y}_{bus}$ to be estimated, corresponding to 36 real values. In addition, here we assume that 4 measurement snapshots are adopted. Therefore, the definitions of the state vector x for the example 9-bus system is shown in Table 4.

Table 4. Definitions of state vector $\boldsymbol{x}$

Row index	Values in the admittance matrix $\boldsymbol{Y}_{bus}$
1 to 9	Real part of off-diagonal values of $\boldsymbol{Y}_{bus}$
10 to 18	Real part of the diagonal values of $\boldsymbol{Y}_{bus}$
19 to 27	Imaginary part of off-diagonal values of $\boldsymbol{Y}_{bus}$
28 to 36	Imaginary part of diagonal values of $\boldsymbol{Y}_{bus}$
37 to 60	Real part of voltage phasors of type 2 buses, snapshot 1 to 4 (6 buses × 4 snapshots)
61 to 84	Imaginary part of voltage phasors of type 2 buses, snapshot 1 to 4 (6 buses × 4 snapshots)

To systematically solve the state vector x in (8), the following optimization problem is formulated,

$$\min_{x} F(x) = \min_{x} \frac{1}{2} \left\| G(\boldsymbol{x}) - \boldsymbol{y} \right\|_2^2 \tag{9}$$

where $\|\bullet\|_2$ represents the L_2 norm of the vector.

Equation (9) can be solved through the Newton's method,

$$\boldsymbol{x}^{w+1} = \boldsymbol{x}^{w} - \boldsymbol{H}_x^{-1}(\boldsymbol{x}^{w}) \cdot \nabla_x F(\boldsymbol{x}^{w}) \tag{10}$$

where $\boldsymbol{H}_x = \partial^2 F(\boldsymbol{x}) / \partial \boldsymbol{x}^2$ is the Hessian matrix of $F(\boldsymbol{x})$, $\nabla_x F(\boldsymbol{x}) = \partial F(\boldsymbol{x}) / \partial \boldsymbol{x}$ is the gradient vector of $F(\boldsymbol{x})$.

In fact, one can observe that it is challenging to derive the analytical expression of $\boldsymbol{H}_x$ and $\nabla_x F(\boldsymbol{x})$. Therefore, here the numerical difference format is utilized to numerically calculate the $\boldsymbol{H}_x$ and $\nabla_x F(\boldsymbol{x})$,

$$\left[\nabla_x F(\boldsymbol{x}^{w})\right]_{k,1} = \left[F(\boldsymbol{x}^{w} + (\boldsymbol{h})_k) - F(\boldsymbol{x}^{w} - (\boldsymbol{h})_k)\right] / (2\Delta x) \tag{11}$$

$$\left[H_x(\boldsymbol{x}^{w})\right]_{j,k} = \begin{bmatrix} F(\boldsymbol{x}^{w} + (\boldsymbol{h})_j + (\boldsymbol{h})_k) \\ -F(\boldsymbol{x}^{w} + (\boldsymbol{h})_j - (\boldsymbol{h})_k) \\ -F(\boldsymbol{x}^{w} - (\boldsymbol{h})_j + (\boldsymbol{h})_k) \\ +F(\boldsymbol{x}^{w} - (\boldsymbol{h})_j - (\boldsymbol{h})_k) \end{bmatrix} \Big/ (4(\Delta x)^2) \tag{12}$$

where $(\boldsymbol{h})_j$ represents a vector whose j^{th} entries is Δx (other entries are zero), Δx is a small perturbation.

III. Numerical Experiments

The proposed method is validated in the IEEE 9-bus test system. The single line view of the system is shown in Figure 3. The IEEE 9-bus system includes 3 generator buses (bus 1, 2, 3), 3 loads, 6 branches and 3 transformers. The available measurements include voltage and current PMU measurements

at bus 1, 2 and 3 (corresponding to buses connected to the power sources), and voltage magnitude measurements at bus 4, 5, 6, 7, 8 and 9, as shown in Table 5. All the branch parameters in the simulation come from Matpower (https://matpower.org/). The number of snapshots for this system is four. The 9-bus system is simulated in PSCAD/EMTDC, and instantaneous measurements are first captured with the standard sampling rate of 80 samples/cycle according to IEC61850-9-2 standard. Afterwards, the voltage and current phasors are extracted according to IEEE C37.118 standard. In fact, the value of admittance matrices could be affected by the operating frequency of the system. Here we assume steady state operation of the system, with the fundamental frequency of 60 Hz.

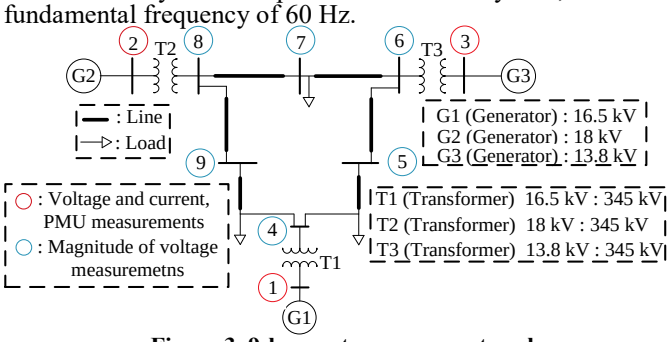

Figure 3. 9-bus system power network

Table 5. Available measurements for the 9-bus system

Bus number	Measurement
1-3 (connected to sources)	Voltage and current, PMU measurements
4-9 (others)	Magnitude of voltage

To validate the performances of our method, the real and imaginary absolute error of the estimated is defined as (*AM* is short for "entry of the admittance matrix"),

$$Real\ AM\ Error(\%) = \frac{|Estimated\ real(AM) - Actual\ real(AM)|}{\sqrt{real(AM)^2 + imag(AM)^2}} \times 100\% \quad (13)$$

$$Imag\ AM\ Error(\%) = \frac{|Estimated\ imag(AM) - Actual\ imag(AM)|}{\sqrt{real(AM)^2 + imag(AM)^2}} \times 100\% \quad (14)$$

A. *Admittance Matrix Estimation*

To simplify the notation, define $\boldsymbol{Y}_{re} = real(\boldsymbol{Y}_{bus})$ and $\boldsymbol{Y}_{im} = imag(\boldsymbol{Y}_{bus})$. The summary of the actual/estimated values of $\boldsymbol{Y}_{re}$ and $\boldsymbol{Y}_{im}$ are shown in Table 6 and Table 7, respectively. The results of other entries of $\boldsymbol{Y}_{bus}$ matrix are not provided since they are always zero due to the network topology. One can observe that the error is very small (the actual and the estimated values are almost the same). The visualization of the absolute errors of $\boldsymbol{Y}_{re}$ and $\boldsymbol{Y}_{im}$ is shown in Figure 4. Here the aforementioned zero entries of the matrices are represented with the white color. The maximum absolute error of the $\boldsymbol{Y}_{re}$ is 0.028%, the maximum absolute error of the $\boldsymbol{Y}_{im}$ is 0.058%. In fact, the authors have verified that the estimated admittance matrix satisfies (2) very accurately. In addition, the authors have substituted the estimated admittance matrix into some applications such as power flow. The results have shown that the estimated admittance matrix enables very accurate power flow results.

Table 6. Actual and estimated values of $\boldsymbol{Y}_{re}$ (unit: p.u.)

Matrix entry	Actual Value	Estimated Value	Matrix entry	Actual Value	Estimated Value
$(\boldsymbol{Y}_{re})_{1,4}$	0.0000	0.0031	$(\boldsymbol{Y}_{re})_{1,1}$	0.0000	0.0032
$(\boldsymbol{Y}_{re})_{2,8}$	0.0000	0.0025	$(\boldsymbol{Y}_{re})_{2,2}$	0.0000	0.0025
$(\boldsymbol{Y}_{re})_{3,6}$	0.0000	0.0035	$(\boldsymbol{Y}_{re})_{3,3}$	0.0000	0.0037
$(\boldsymbol{Y}_{re})_{4,5}$	-1.9422	-1.9415	$(\boldsymbol{Y}_{re})_{4,4}$	3.3074	3.3057
$(\boldsymbol{Y}_{re})_{4,9}$	-1.3652	-1.3624	$(\boldsymbol{Y}_{re})_{5,5}$	3.2242	3.2277
$(\boldsymbol{Y}_{re})_{5,6}$	-1.2820	-1.2837	$(\boldsymbol{Y}_{re})_{6,6}$	2.4371	2.4405
$(\boldsymbol{Y}_{re})_{8,9}$	-1.1876	-1.1883	$(\boldsymbol{Y}_{re})_{7,7}$	2.7722	2.7694
$(\boldsymbol{Y}_{re})_{7,8}$	-1.6171	-1.6156	$(\boldsymbol{Y}_{re})_{8,8}$	2.8047	2.8118
$(\boldsymbol{Y}_{re})_{7,6}$	-1.1551	-1.1575	$(\boldsymbol{Y}_{re})_{9,9}$	2.5528	2.5563

Table 7. Actual and estimated values of $\boldsymbol{Y}_{im}$ (unit: p.u.)

Matrix entry	Actual Value	Estimated Value	Matrix entry	Actual Value	Estimated Value
$(\boldsymbol{Y}_{im})_{1,4}$	17.361	17.364	$(\boldsymbol{Y}_{im})_{1,1}$	-17.361	-17.370
$(\boldsymbol{Y}_{im})_{2,8}$	16.000	16.008	$(\boldsymbol{Y}_{im})_{2,2}$	-16.000	-16.001
$(\boldsymbol{Y}_{im})_{3,6}$	17.065	17.052	$(\boldsymbol{Y}_{im})_{3,3}$	-17.065	-17.057
$(\boldsymbol{Y}_{im})_{4,5}$	10.511	10.515	$(\boldsymbol{Y}_{im})_{4,4}$	-39.301	-39.292
$(\boldsymbol{Y}_{im})_{4,9}$	11.604	11.597	$(\boldsymbol{Y}_{im})_{5,5}$	-15.841	-15.840
$(\boldsymbol{Y}_{im})_{5,6}$	5.5882	5.5884	$(\boldsymbol{Y}_{im})_{6,6}$	-32.154	-32.144
$(\boldsymbol{Y}_{im})_{8,9}$	5.9751	5.9776	$(\boldsymbol{Y}_{im})_{7,7}$	-23.303	-23.290
$(\boldsymbol{Y}_{im})_{7,8}$	13.698	13.704	$(\boldsymbol{Y}_{im})_{8,8}$	-35.445	-35.427
$(\boldsymbol{Y}_{im})_{7,6}$	9.7842	9.7879	$(\boldsymbol{Y}_{im})_{9,9}$	-17.338	-17.349

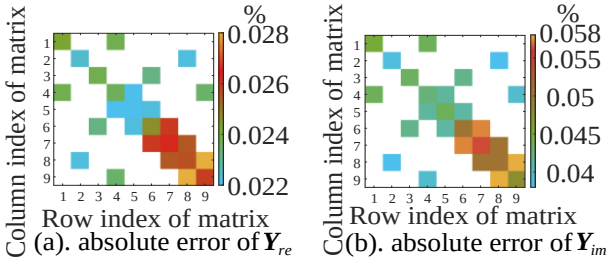

Figure 4. Absolute error of $\boldsymbol{Y}_{re}$ and $\boldsymbol{Y}_{im}$, 9-bus system

B. *Robustness towards Measurement Errors*

To validate the practicability of the proposed method, the effect of measurement errors is studied. The measurement errors are selected as follows. The Gaussian noises with zeros mean and 0.8% standard deviation are added to the voltage magnitude measurements [14]. Gaussian noises with zeros mean and 0.01% standard deviation are added to the PMU phasor measurements respectively [14]. Due to space limitation, here we only show the visualization of absolute errors of $\boldsymbol{Y}_{re}$ and $\boldsymbol{Y}_{im}$ show in Figure 5. The maximum absolute error of the $\boldsymbol{Y}_{re}$ is around 0.26%, and the maximum absolute error of the $\boldsymbol{Y}_{im}$ is 0.25%.

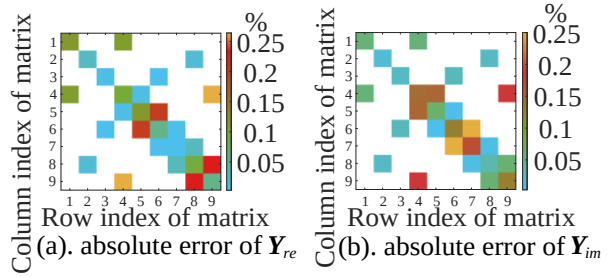

Figure 5. Absolute error of $\boldsymbol{Y}_{re}$ and $\boldsymbol{Y}_{im}$, 9-bus system, with measurement errors

Since the noises of PMU measurements and voltage magnitude measurements are random values, the robustness of the proposed admittance matrix estimation method towards measurements may not be properly evaluated based on one

single scenario. To further evaluate the performance of the proposed method considering random noises, a large number of scenarios are generated and the average of the maximum absolute errors of the $\boldsymbol{Y}_{re}$ and $\boldsymbol{Y}_{im}$ are shown in Table 8. One can observe that the maximum error is less than 0.34%, proving the robustness of the proposed method towards measurement errors.

Table 8. Average of the maximum absolute errors of $\boldsymbol{Y}_{re}$ and $\boldsymbol{Y}_{im}$, with large number of scenarios

Number of Scenario	Average maximum absolute error of $\boldsymbol{Y}_{re}$	Average maximum absolute error of $\boldsymbol{Y}_{im}$
5	0.22%	0.24%
10	0.31%	0.27%
20	0.34%	0.21%
50	0.27%	0.29%
100	0.25%	0.31%

C. *Additional Experiments on 118-Bus System*

To further validate the effectiveness of the proposed method in large systems, the IEEE 118-bus system is studied in this section. The system includes 28 generator buses, 90 loads. 179 branches and 9 transformers. Same as the 9-bus system, the available measurements include voltage and current PMU measurements at generator buses, and voltage magnitude measurements at other buses. All the branch parameters in the simulation come from Matpower (https://matpower.org/) . The number of snapshots for this system is four.

The visualization of the absolute error of $\boldsymbol{Y}_{re}$ and $\boldsymbol{Y}_{im}$ is shown in Figure 6. Here the zero entries of the matrices (due to the network topology) are represented with the white color. The maximum absolute error of the $\boldsymbol{Y}_{re}$ is 0.015%, the maximum absolute error of the $\boldsymbol{Y}_{im}$ is 0.040%. The estimation results with the larger systems are of the similar accuracy as the 9-bus system.

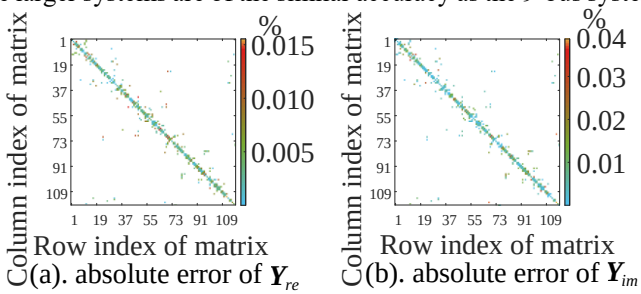

(a). absolute error of $\boldsymbol{Y}_{re}$ (b). absolute error of $\boldsymbol{Y}_{im}$

Figure 6. Absolute error of $\boldsymbol{Y}_{re}$ and $\boldsymbol{Y}_{im}$, 118-bus system

D. *Comparison to Other Methods*

This session compares the proposed method to some existing methods, including the Carson's method [15], the admittance matrix estimation method [12] and the conventional two-terminal line parameters estimation method [7].

First, the Carson's equation was widely adopted to directly calculate line parameters. This method requires accurate physical parameters including wires conductivity, permeability, geometric spacing among wires, ground resistivity, etc. However, some of these physical parameters are hard to be accurately obtained as they can vary with different weather and operating conditions.

Second, for methods that estimate parameters from available measurements, compared to the existing admittance matrix estimation method [12], the number of PMUs can be much reduced using the proposed method. Compared to the existing conventional two-terminal line parameter estimation method [7], the proposed method can directly estimate the entire admittance matrix instead of branch parameters, and does not require current measurements on type 2 buses.

IV. Conclusion

This paper proposes a novel admittance matrix estimation method on power networks based on hybrid measurements. The proposed method only needs to install a few PMUs at key buses while placing voltage magnitude measurements at the rest of the buses. To work with the hybrid measurements, the proposed method formulates a new model of the power networks, and utilize Newton's method to solve the unknown admittance matrix of the system. Numerical experiments prove that the proposed method can accurately and reliably estimate the admittance matrix. In addition, this method presents robustness towards measurement errors.

Reference

[1] L. Hofmann, "Series expansions for line series impedances considering different specific resistances, magnetic permeabilities, and dielectric permittivities of conductors, air, and ground," *IEEE Trans. Power Del.*, vol. 18, no. 2, pp. 564–70, Apr. 2003.

[2] H. Keshtkar, S. Khushalani Solanki, and J. Solanki, "Improving the accuracy of impedance calculation for distribution power system," *IEEE Trans. Power Del*., vol. 29, no. 2, pp. 570–579, Apr. 2014.

[3] G. L. Kusic and D. L. Garrison, "Measurement of transmission line parameters from SCADA data," in *Proc. IEEE PES Power Syst. Conf. Expo.*, vol. 1, Oct. 2004, pp. 440–445.

[4] Y. Wang and W. Xu, "Algorithms and field experiences for estimating transmission line parameters based on fault record data," *IET Gener. Transm. Distrib*, vol. 9, no. 13, pp. 1773–1781, 2015.

[5] G. Sivanagaraju, S. Chakrabarti and S. C. Srivastava, "Uncertainty in Transmission Line Parameters: Estimation and Impact on Line Current Differential Protection," *IEEE Trans. Instrum. Meas.*, vol. 63, no. 6, pp. 1496-1504, June 2014.

[6] Ren P , Lev-Ari H , Abur A . "Tracking Three-Phase Untransposed Transmission Line Parameters Using Synchronized Measurements, " *IEEE Trans Power Syst*., vol. 33, no. 4, pp. 4155-4163, July 2018.

[7] V. Milojević, S. Čalija, G. Rietveld, M. V. Ačanski and D. Colangelo, "Utilization of PMU Measurements for Three-Phase Line Parameter Estimation in Power Systems," *IEEE Trans Instrum. Meas.*, vol. 67, no. 10, pp. 2453-2462, Oct. 2018.

[8] M. Asprou and E. Kyriakides, "Estimation of transmission line parameters using PMU measurements," *IEEE Power Energy Soc. Gen. Meet. (PESGM)*, Denver, CO, 2015, pp. 1-5.

[9] M. Asprou and E. Kyriakides, "Identification and Estimation of Erroneous Transmission Line Parameters Using PMU Measurements," *IEEE Trans Power Del.*, vol. 32, no. 6, pp. 2510-2519, Dec. 2017.

[10] P. A. Pegoraro, K. Brady, P. Castello, C. Muscas and A. von Meier, "Line Impedance Estimation Based on Synchrophasor Measurements for Power Distribution Systems," *IEEE Trans Instrum. Meas.*, vol. 68, no. 4, pp. 1002-1013, April 2019.

[11] M. R. M. Castillo, J. B. A. London and N. G. Bretas, "An approach to power system branch parameter estimation," *IEEE Canada Elect. Power Conf., Vancouver, BC*, 2008, pp. 1-5.

[12] O. Lateef, R. G. Harley and T. G. Habetler, "Bus Admittance Matrix Estimation Using Phasor Measurements," *IEEE Power Energy Soc. Innovative Smart Grid Technologies Conf.* (ISGT), Washington, DC, USA, 2019, pp. 1-5.

[13] M. Saadeh, M. Alsarray and R. McCann, "Estimation of the bus admittance matrix for transmission systems from synchrophasor data," *IEEE/PES Trans. Distrib. Conf. and Expo. (T&D)*, Dallas, TX, 2016, pp. 1-5.

[14] M. Nejati, N. Amjady, and H. Zareipour, "A new stochastic search technique combined with scenario approach for dynamic state estimation of power systems," *IEEE Trans. Power Syst.*, vol. 27, no. 4, pp. 2093–2105, Nov. 2012.

[15] J. R. Carson, "Wave propagation in overhead wires with earth return," Bell Syst. Tech. J., vol. 7, pp. 11–25, 1928.